Proc. Natl. Acad. Sci. USA
Vol. 88, pp. 5307–5311, June 1991
Biochemistry

Crystal structure of [Leu^1]zervamicin, a membrane ion-channel peptide: Implications for gating mechanisms

(x-ray diffraction/channel mouth/helix bending/polymorphs/α-alkyl amino acids)

ISABELLA L. KARLE*, JUDITH L. FLIPPEN-ANDERSON*, SANJAY AGARWALLA†, AND PADMANABHAN BALARAM†

*Laboratory for the Structure of Matter, Naval Research Laboratory, Washington, DC 20375-5000; and †Molecular Biophysics Unit, Indian Institute of Science, Bangalore 560 012, India

Contributed by Isabella L. Karle, March 21, 1991

ABSTRACT **Structures in four different crystal forms of [Leu^1]zervamicin (zervamicin Z-L, Ac-Leu-Ile-Gln-Iva-Ile^5-Thr-Aib-Leu-Aib-Hyp^{10}-Gln-Aib-Hyp-Aib-Pro^{15}-Phol, where Iva is isovaline, Aib is α-amino isobutyric acid, Hyp is 4-hydroxyproline, and Phol is phenylalaninol), a membrane channel-forming polypeptide from *Emericellopsis salmosynnemata*, have been determined by x-ray diffraction. The helical structure is amphiphilic with all the polar moieties on the convex side of the bent helix. Helices are bent at Hyp^{10} from ≈30° to ≈45° in the different crystal forms. In all crystal forms, the peptide helices aggregate in a similar fashion to form water channels that are interrupted by hydrogen bonds between N$^{\epsilon}$H(Gln^{11}) and O$^{\delta}$(Hyp^{10}) of adjacent helices. The Gln^{11} side chain is folded in an unusual fashion in order to close the channel. Space is available for an extended conformation for Gln^{11}, in which case the channel would be open, suggesting a gating mechanism for cation transport. Structural details are presented for one crystal form derived from methanol/water solution: $C_{85}H_{140}N_{18}O_{22}\cdot 10H_2O$, space group $P2_1$, a = 23.068(6) Å, b = 9.162(3) Å, c = 26.727(9) Å, β = 108.69(2)° (standard deviation of last digit is given in parentheses); overall agreement factor R = 10.1% for 5322 observed reflections [$|F_o| > 3\sigma(F)$]; resolution, 0.93 Å.**

Several acyclic, α-aminoisobutyric acid (Aib)-containing polypeptides of fungal origin (Fig. 1) form voltage-gated channels in phospholipid bilayer membranes (1–6). The best studied members of this class are alamethicins, 20-residue peptides for which a crystal structure has been reported at 1.5-Å resolution (3). Several models for alamethicin ion channels have been proposed (3–6), based on the helical conformation observed in crystals. The molecular packing in alamethicin crystals, however, did not directly provide a model for a membrane-phase channel aggregate (3). The zervamicins are a related class of peptides isolated from cultures of *Emericellopsis salmosynnemata* (7). These peptides are shorter (16 residues) than alamethicin and contain several polar residues (Thr, Gln, Hyp) distributed evenly throughout the sequence (8). A preliminary report suggests that zervamicins exhibit lower pore-forming ability and enhanced antibacterial properties compared with alamethicin (8). More recently, the zervamicins have been shown to form voltage-dependent multilevel ion channels in bilayer membranes (ref. 9; M. S. P. Sansom, personal communication). Although the conductive activity is qualitatively similar to that of alamethicin, the kinetics of switching between states is appreciably faster for zervamicins. The major polypeptide components of zervamicin (IIA and IIB) contain a Trp residue at position 1. During HPLC fractionation, a minor component containing Leu at position 1, [Leu^1]zervamicin (zervamicin Z-L), has been isolated. The component has been crystallized and the structure determined in four different crystal forms to resolutions as high as 0.93 Å and R = 10.1% (Table 1). In each of the four different crystal forms, space groups $P2_1$ and $P2_12_12_1$, the peptide molecules associate to form similar discontinuous water channels, which appear to give further insights into the nature of an ion channel, a possible gating mechanism, and the dynamics of a bent helix molecule.

Alamethicin I (II)	Ac-Aib-Pro-Aib-Ala-Aib^5-Ala(Aib)-Gln-Aib-Val-Aib^{10}-Gly-Leu-Aib-Pro-Val^{15}-Aib-Aib-Glu-Gln-Phol^{20}
Antiamoebin I (II)	Ac-Phe-Aib-Aib-Aib-D-Iva^5-Gly-Leu-Aib-Aib-Hyp^{10}-Gln-D-Iva-Hyp(Pro)-Aib-Pro^{15}-Phol
Zervamicin IIA (IIB)	Ac-Trp-Ile-Gln-Aib(Iva)-Ile^5-Thr-Aib-Leu-Aib-Hyp^{10}-Gln-Aib-Hyp-Aib-Pro^{15}-Phol
Zervamicin Z-L	Ac-Leu-Ile-Gln-Iva-Ile^5-Thr-Aib-Leu-Aib-Hyp^{10}-Gln-Aib-Hyp-Aib-Pro^{15}-Phol

FIG. 1. Sequences of some Aib-containing antibiotics that transport ions across membranes. Phol, phenylalaninol; Iva, isovaline (α-ethylalanine); Hyp, 4-hydroxyproline.

EXPERIMENTAL PROCEDURES

[Leu^1]Zervamicin was isolated from a heterogeneous zervamicin mixture by HPLC on a reverse-phase C_{18} column, as described (10). Crystals were grown by slow evaporation of methanol/water solution or by vapor diffusion of water into ethylene glycol/ethanol solutions containing about 3 mg of peptide in 0.4 ml of solvent. X-ray diffraction data were measured with a four-circle automated diffractometer with CuK_α radiation on crystals under the conditions listed in Table 1 for a best set of data. Lowering the temperature for some of the crystal forms resulted in shattering the crystal. Rapid scan speeds, 7–15°/min, were used in order to collect most of the data before significant deterioration of the crystal. The structures were solved by a vector-search procedure (11) contained in the SHELX84 package of programs (MicroVAX version of the SHELXTL system of programs; Siemens Instruments, Madison, WI). The search model was based on the backbone atoms of the known structure of a 16-residue apolar analog of zervamicin (12) and was followed by a partial-structure procedure (13) by which the atoms in the side chains were located. The detailed structure only of crystal A will be reported here. Full-matrix anisotropic least-squares refine-

The publication costs of this article were defrayed in part by page charge payment. This article must therefore be hereby marked "*advertisement*" in accordance with 18 U.S.C. §1734 solely to indicate this fact.

Abbreviations: Aib, α-aminoisobutyric acid (α-methylalanine); Hyp, 4-hydroxyproline; Iva, isovaline (α-ethylalanine); Phol, phenylalaninol.

Table 1. Crystal parameters for Ac-Leu-Ile-Gln-Iva-Ile-Thr-Aib-Leu-Aib-Hyp-Gln-Aib-Hyp-Aib-Pro-Phol, $C_{85}H_{140}N_{18}O_{22}{\cdot}xH_2O$

Parameter	Crystal A*†	Crystal B†	Crystal C	Crystal D
Space group	$P2_1$	$P2_1$	$P2_12_12_1$	$P2_12_12_1$
Cell dimensions				
a, Å	23.068(6)	21.857(4)	10.337(2)	10.160(3)
b, Å	9.162(3)	9.381(3)	28.389(7)	28.252(9)
c, Å	26.727(9)	26.744(6)	39.864(11)	40.338(9)
β, degrees	108.69(2)	105.22(2)	90	90
Growth solvent	CH_3OH/H_2O	CH_3OH/H_2O	$HOCH_2CH_2OH$	‡
No. of reflections				
$[\|F_o\| > 3\sigma(F)]$	5322	2939	4239	2251
Crystal condition	−45°C, dry	20°C, dry	20°C, in capillary	20°C, in capillary
Volume per asymmetric unit, Å^3	2676	2638	2924	2895

*$R = \Sigma||F_o| - |F_c||/\Sigma|F_o|$ for all data with $|F_o| > 3\sigma(F) = 10.1\%$; resolution, 0.93 Å. Estimated SDs for backbone: ≈0.023 Å (bonds); ≈1.3° (angles). Estimated SDs for side chains: ≈0.03 Å (bonds); ≈1.7° (angles).

†Crystals A and B were present in the same crystallizing vial.

‡Crystal D was obtained by soaking crystal C in aqueous KCl (no K^+ in crystal D); approximate coordinates for the peptide are known, but least-squares refinement was not completed.

ment was performed on the C, N, and O atoms in the peptide, after which H atoms were placed in idealized positions with C–H distances of 0.96 Å and allowed to ride with the C or N atoms to which each was bonded for the final cycles of refinement. The thermal factors for the H atoms were fixed at $U_{iso} = 0.125$. Water molecules for a total of 11 sites (one pair of sites is mutually exclusive) were located in a series of difference maps and added stepwise to the refinement. The phenyl group in the Phol residue was constrained to be a regular hexagon with C–C distances of 1.395 Å, although the position and orientation of the hexagon and the isotropic thermal values for each atom in the hexagon were subjected to least-squares refinement. Finally, the amide moiety in the Gln^3 side chain, particularly the N$^{\varepsilon}$(3) atom (in all the crystal forms) was particularly mobile; therefore the bond lengths and bond angles in the -C(O)NH$_2$ moiety were constrained to reasonable values while the orientation of the amide group and the isotropic thermal factors associated with the C$^{\delta}$(3), O$^{\varepsilon}$(3), and N$^{\varepsilon}$(3) atoms were allowed to vary in the least-squares process. With the above constraints, and not quite a full sphere of data to a resolution of 0.93 Å due to the onset of crystal deterioration, the final R factor is 10.1% for 5322 data observed with $|F_o| > 3\sigma(F)$. Bond lengths and bond angles (estimated SD, approximately 0.02 Å for bonds and 1.2° for angles) do not show significant or systematic differences from expected values.‡

RESULTS

The Peptide Helix. Both alamethicin and zervamicin have a high proportion of Aib residues, which are strong helix formers (14–16). Zervamicin has polar moieties in residues 3, 6, 10, 11, 13, and 16. As expected for a helical structure with polar residues spaced at each third or fourth position (17, 18), all of these polar moieties are on one side of the zervamicin helix (Fig. 2), thus giving the helix an amphiphilic character. Although Gln^{11} would appear to break the rule, the torsions about the C$^{\alpha}$—C$^{\beta}$ and C$^{\beta}$—C$^{\delta}$ bonds in Gln^{11} are −51° and −55°, respectively, which fold the polar -C(O)NH$_2$ group back from the nonpolar face to the polar face of the helix. The unusual conformation and the probable mobility of the Gln^{11} side chain strongly suggest the location of the gating mechanism during ion transport (see below). Additionally, the polar face is enhanced by the exposed backbone carbonyl oxygens in residues 6, 7, and 10, which do not participate in intrahelical hydrogen bonds (Table 2) due to the presence of Hyp^{10} and Hyp^{13}. These carbonyls are available for hydrogen bonding to the neighboring water molecules or another peptide molecule or for making transient ligands with cations that are being transported.

Despite the presence of two Hyp residues and one Pro residue, the backbone is entirely helical. Torsional angles are listed in Table 3. An α-helix is formed from the amino terminus through the ninth residue. A β-ribbon containing Hyp^{10}, Hyp^{13}, and Pro^{15} is twisted into a helix that extends to the carboxyl terminus. The helix is bent at Hyp^{10}, giving the peptide an overall banana shape. It is interesting that the

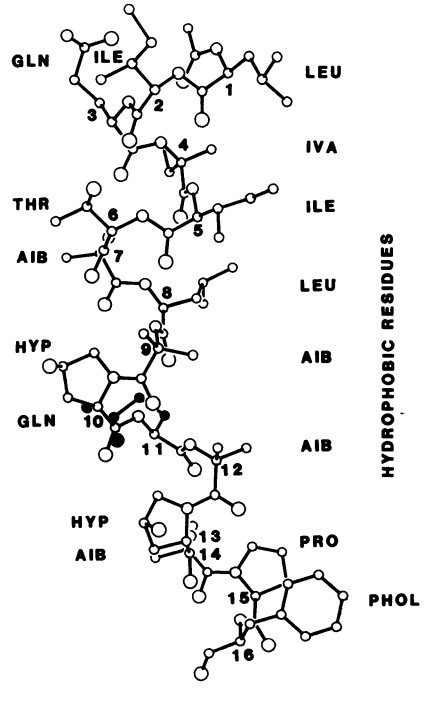

FIG. 2. Conformation of [Leu^1]zervamicin drawn with the coordinates obtained from crystal A. The C$^{\alpha}$ atoms are labeled 1–16. The side chain in Gln^{11} (filled circles) is not extended to the hydrophobic face but folded backward to the polar face of the helix.

‡Supplementary material consisting of atomic coordinates for C, N, and O atoms, bond lengths and angles, anisotropic thermal factors, and coordinates for hydrogen atoms has been deposited with the Cambridge Structural Data Base, University Chemical Laboratory, Lensfield Road, Cambridge CB2 IEW, U.K. Lists of observed and calculated structure factors are available from I.L.K. and J.L.F.-A.

Table 2. Hydrogen bonds

Peptide helix						Water structure		
Type	Donor	Acceptor	N · · · O or O · · · O, Å	H · · · O,* Å	C=O · · · N angle, degrees	Donor	Acceptor	N · · · O or O · · · O,* Å
Head-to-tail	N(1)	O(15)†	2.93	2.04	122	W(1)	$O^{\gamma}(6)$§	2.82
	N(2)	O(16)†	2.96	2.07	140	W(1)	O(10)	3.00
Intramolecular	N(3)	$O^{\epsilon}(3)$	3.07	2.32		W(2)	O(3)‡	2.91
5 → 1	N(4)	O(0)	2.85	2.01	167	W(2)	W(1)	2.82
	N(5)	O(1)	3.15	2.26	158	W(3)	$O^{\delta}(13)$	3.21
	N(6)	O(2)	3.25	2.40	146	W(3)	W(2)	2.82
Intramolecular	$O^{\gamma}(6)$	O(2)	2.79	1.97		W(4A)	W(3)	2.50
5 → 1	N(7)	O(3)	2.88	2.03	155	W(4B)	W(3)	2.89
	N(8)	O(4)	3.36	2.60	131	$N^{\epsilon}(3)$§	W(4B)	3.08
	N(9)	O(5)	2.98	2.26	165	W(5)	W(4A)	2.98
Intermolecular	$O^{\delta}(10)$‡	O(7)	2.75	1.91		W(5)	W(6)	3.08
	$N^{\epsilon}(11)$§	O(6)	3.09	2.22		W(6)	O(14)	2.90
	$N^{\epsilon}(11)$§	$O^{\delta}(10)$	2.91	2.06		W(6)†	$O^{\epsilon}(3)$	2.73
β-Ribbon	N(11)	O(8)	2.88	2.01	138	O(16)	W(6)	2.67
	N(12)	O(9)	3.15	2.26	124	W(7)	W(5)	2.48
Intermolecular	$O^{\delta}(13)$	$O^{\epsilon}(11)$¶	2.67	1.85		W(8)	O(11)	3.00
β-Ribbon	N(14)	O(11)	3.01	2.12	129	W(8)	W(9)†	2.67
	N(16)	O(13)	2.82	1.99	129	W(9)	O(12)‖	2.94
						W(9)	W(8)	3.13
						W(10)	O(15)	3.15

*The H atoms were placed in idealized positions with the N–H distance equal to 0.96 Å.
†Symmetry equivalents $1 + x, y, 1 + z$ to coordinates listed in supplementary material (see footnote at end of *Experimental Procedures*).
‡Symmetry equivalents $2 - x, -\frac{1}{2} + y, 1 - z$.
§Symmetry equivalents $2 - x, \frac{1}{2} + y, 1 - z$.
¶Symmetry equivalents $x, 1 + y, z$.
‖Symmetry equivalents $x, -1 + y, z$.

conformation of the backbone of a completely apolar synthetic analog of [Trp^1]zervamicin (12) is almost identical to that of the backbone in the natural [Leu^1]zervamicin. The configuration of the Iva residue at position 4 is *R*, confirming an earlier stereochemical assignment (8).

Channel Formation. The peptide molecules in all four polymorphs have very similar helical conformations, intramolecular hydrogen bonds, head-to-tail hydrogen bonds, and interpeptide hydrogen bonds. The differences in conformation are manifested mainly by the bend of the helix, 36° for A, 30° for B, and 45° for C (structure D is not sufficiently well refined at this time for us to make a measurement). In all the crystals, the polar faces associate in a common antiparallel fashion. Fig. 3 illustrates this association with a superposition of the envelopes of the structures, showing the peptide molecules A, B, and C. In the middle, the molecules in each

Table 3. Torsion angles* (degrees)

Residue	ϕ	ψ	ω	χ^1	χ^2	χ^3	χ^4
Leu^1	−51†	−45	−173	175	73, −169		
Ile^2	−63	−45	−178	164, −68	168		
Gln^3	−69	−40	−172	−67	85	15, −139‡	
Iva^4	−57	−54	−177	57			
Ile^5	−74	−35	176	172, −66	180		
Thr^6	−59	−44	−176	−64, 179§			
Aib^7	−59	−37	−171				
Leu^8	−91	−24	−171	−74	−75, 165		
Aib^9	−55	−39	−179				
Hyp^{10}	−63	−16	−177	−24	36	−35	19¶
Gln^{11}	−89	−9	179	−51	−54	−44, 135‖	
Aib^{12}	−51	−37	−177				
Hyp^{13}	−77	−6	−168	−21	34	−33	20**
Aib^{14}	−53	−44	−178				
Pro^{15}	−80	−13	−170	−10	24	−29	22††
$Phol^{16}$	−115	+72‡‡		−69	−75, 101		

The torsion angles for rotation about the bonds of the peptide backbone (ϕ, ψ, and ω) and about bonds of the amino acid side chains (χ^n) are described in ref. 19.
*Estimated SDs, ≈1.5°.
†C′(O),N(1),C^{α}(1),C′(1).
‡C^{β}(3),C^{γ}(3),C^{δ}(3),O^{ϵ}(3), +15°; C^{β}(3),C^{γ}(3),C^{δ}(3),N^{ϵ}(3), −139°.
§N(6),C^{α}(6),C^{β}(6),O^{γ}(6), −64°; N(6),C^{α}(6),C^{β}(6), C^{γ}(6), 179°.
¶C^{δ}(10),N(10),C^{α}(10),C^{β}(10), 3°; C^{α}(10),C^{β}(10),C^{γ}(10),O^{δ}(10), −81°.
‖C^{β}(11),C^{γ}(11),C^{δ}(11),O^{ϵ}(11), −44°; C^{β}(11),C^{γ}(11),C^{δ}(11), N^{ϵ}(11), 135°.
**C^{δ}(13),N(13),C^{α}(13),C^{β}(13), 1°; C^{α}(13),C^{β}(13),C^{γ}(13),O^{δ}(13), −83°.
††C^{δ}(15),N(15),C^{α}(15),C^{β}(15), −8°.
‡‡N(16),C^{α}(16),C(16)(CH_2OH),O(16)(CH_2OH).

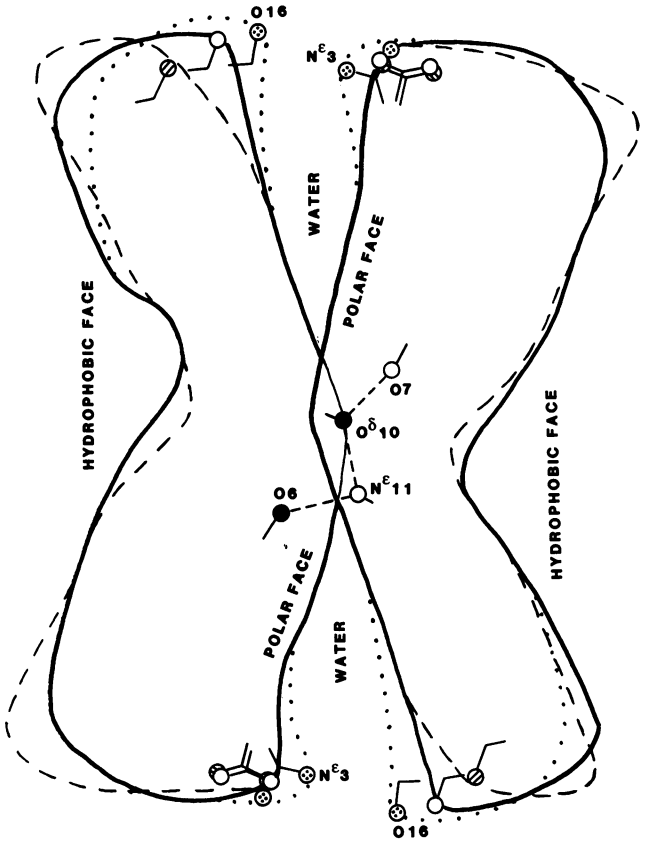

FIG. 3. Schematic diagram showing a superposition of the envelopes of [Leu^1]zervamicin helices in crystal A (solid line), crystal B (dotted line), and crystal C (dashed line). The polar face of the helices associates in an antiparallel fashion and forms a discontinuous water channel that contains a different number of water molecules in each crystal form. The channel is closed in the middle by *inter*peptide hydrogen bonds involving backbone carbonyls O(6) and O(7) and side chain moieties O$^{\delta}$(Hyp^{10}) and N$^{\varepsilon}$(Gln^{11}). The size of the mouth of the channel is determined by the movement of O(Phol^{16}) and N$^{\varepsilon}$(Gln^3) in adjacent peptide molecules.

crystal are held together with *inter*peptide hydrogen bonds O(Thr^6) · · · N$^{\varepsilon}$(Gln^{11}), N$^{\varepsilon}$(Gln^{11}) · · · O$^{\delta}$(Hyp^{10}), and O$^{\delta}$(Hyp^{10}) · · · O(Aib^7). The banana-shaped molecules spread apart from each other at either end by differing amounts, related to the bend in each helix. The resulting cavities are filled with varying amounts of water depending upon the size of the cavity. For crystal A there are eight water sites (one disordered) at each end. These are shown in detail in Fig. 4, along with the hydrogen bonding between water molecules and between peptide and water molecules.

The mouth of the water cavity is constricted or expanded depending upon the bend in the helix. The O(Phol^{16}) · · · N$^{\varepsilon}$(Gln^3) separation is 3.7 Å in crystal B, 6.8 Å in crystal A, and >8 Å in crystal C. Despite the flexibility of the peptide, atom O(Phol^{16}) is relatively rigid since it participates in head-to-tail hydrogen bonding. The -C(O)NH$_2$ end of Gln^3, however, is quite mobile and N$^{\varepsilon}$(3) makes hydrogen bonds mainly to disordered or transient water sites. The carbonyl O(3) makes an *intra*helical hydrogen bond to the backbone N(3) moiety of the same residue in crystal A but not in crystal B.

Gating. A continuous water channel is not formed between the polar surfaces of adjacent peptide molecules. A view of the middle segments of adjacent molecules, where *inter*peptide hydrogen bonding takes place and closes the channel, is shown in Fig. 5. The view is perpendicular to that in Figs. 3 and 4 and is directed into the helices. Three molecules appear to define the closed channel. The side chain of Gln^{11} is not

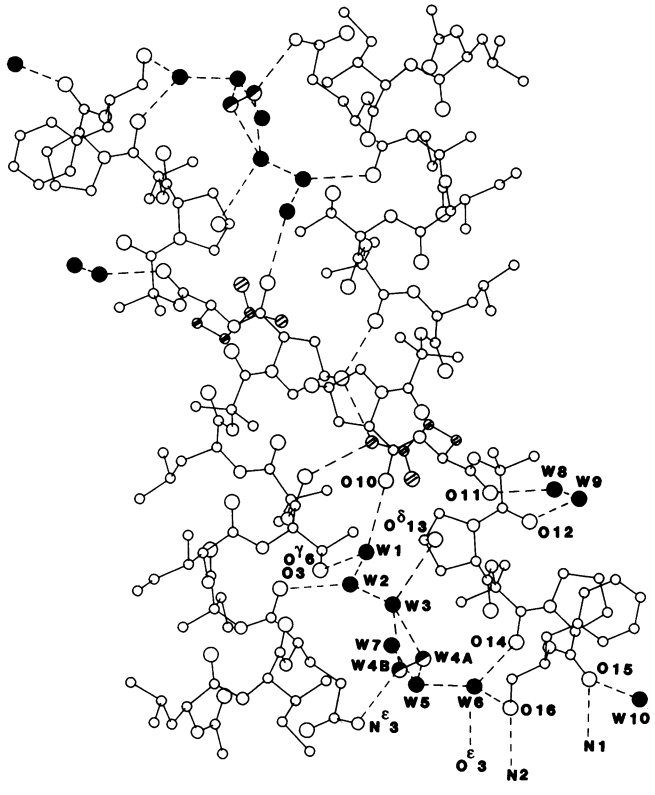

FIG. 4. Water molecules (●) in crystal A of [Leu^1]zervamicin. The two peptide molecules are related by a twofold screw axis. The atoms in the side chain of Gln^{11} are marked with stripes. Hydrogen bonds are indicated by dashed lines.

extended as Gln^7 of alamethicin (3) but is folded backward to form a hydrogen bond with O$^{\delta}$(Hyp^{10}). The Hyp residue is quite rigid. It is conceivable that under the application of a potential, the Gln^{11} side chain can open the channel by

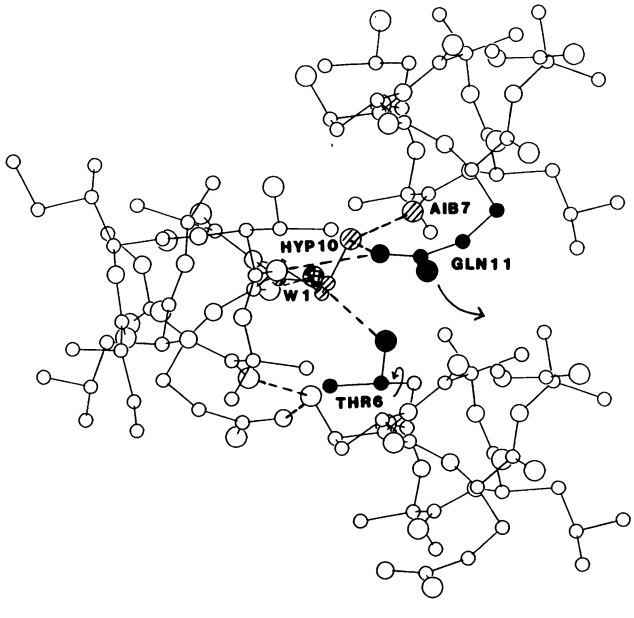

FIG. 5. A possible gating mechanism by Gln^{11} and Thr^6 in channels formed by [Leu^1]zervamicin. The view of the closed channel is perpendicular to the orientation in Figs. 3 and 4. Only the middle residues of three adjacent peptide molecules are shown. The water molecule closest to the closed portion of the channel is W(1) (checkered). The carbonyl oxygen in Aib^7 and the hydroxyl in Hyp^{10} (striped) are relatively rigid moieties and may define a boundary of a hypothetical open channel.

rotating into the adjacent space at the right (Fig. 5). If a column of water is pushed through the channel in a single file by a cation (20), it may also be possible that the side chain in Thr^6 can rotate about the C^α—C^β bond to further enlarge the channel. As shown in Fig. 4, there are many carbonyl, hydroxyl, and amino moieties along the channel to provide ligands for a cation that is being transported.

Nonpolar Face of Helix. Helical peptides forming a channel across a membrane would have their nonpolar side facing the membrane. The molecular recognition and aggregation of apolar helical peptides are not particularly selective. Such helical peptides have been found to crystallize with the helix axes either in an all-parallel motif or in an antiparallel motif. Even peptides with the same sequence have either all-parallel or antiparallel aggregation in different crystal forms (21, 22). Similarly in [Leu^1]zervamicin, in crystals A and B (space group $P2_1$), the nonpolar face of the helix associates in an antiparallel fashion, while in crystals C and D (space group $P2_12_12_1$), the nonpolar face associates in a parallel fashion. The inference can be drawn that the nonpolar face is also fairly insensitive to the helix axis direction with respect to the membrane.

DISCUSSION

[Leu^1]zervamicin is a bent helical molecule, 29 Å long, with all the polar side chains on the convex side and the nonpolar side chains on the concave side. Alamethicin (3), also a bent helix, has a much smaller degree of bending and has fewer polar moieties on the convex face (Fig. 1). The helix in both peptides is flexible as shown by different amounts of bending in the three conformers in the same crystal of alamethicin and the four conformers in four different polymorphs of [Leu^1]-zervamicin. Although complex irregular water channels were observed in the alamethicin crystals, the polar residues are not directed toward the center of the channel as might be expected for a membrane ion channel (3). In each of the four crystal forms of [Leu^1]zervamicin, the polar faces of adjacent peptide molecules form the boundary of a water channel.

The molecular recognition of the nonpolar side of [Leu^1]zervamicin is not very specific. Either parallel or antiparallel association takes place in the different crystal forms. In contrast, the polar face is very specific in forming an antiparallel association with an adjacent molecule and a hydrogen bond between Hyp^{10} and Gln^{11}, among others. The $Hyp^{10} \cdots Gln^{11}$ hydrogen bond interrupts the water channel. The remarkable observation is that the Gln^{11} side chain has to reverse its direction, in a swinging-arm fashion, to approach the Hyp^{10} of an adjacent, antiparallel peptide. It may be indicative of the gating mechanism in ion transport under the application of a potential. The size of the water channel near its interruption is restricted to one water molecule or one cation. The implications from the crystal structure analyses are that the water channel is not an open channel—i.e., that there is no passive diffusion of cations. This point has been emphasized further by soaking crystals in KCl solution for various times at various concentrations. Short of the crystal cracking and disintegrating, the soaking produced crystals with somewhat different cell parameters, but with no K^+ penetration.

Time-resolved fluorescence anisotropy measurements on helical bilayer-spanning 21-residue peptides have shown that the amplitude of fast fluctuations are largest at the helix ends and decrease toward the center of the helix (23). The four crystal structures show an expansion or constriction of the mouth of the channel, $O(16) \cdots Gln^3$, that varies from 3.7 Å to >8.0 Å. The cation may be trapped in the channel by constriction of the mouth (24).

One of the interesting implications of the crystal structure of [Leu^1]zervamicin is the role played by the mobility of the long side chain of Gln residues: the demonstrated mobility of Gln^3 in controlling the size of the mouth of the water channel, and the implied mobility of Gln^{11} (by its unusual conformation) in probable participation in the gating mechanism. For proteins, the role of Gln residues has been characterized as relatively indifferent and has no extreme properties or violent preferences (25). Perhaps one of the distinctive functions of this residue is in the regulation of ion-transport peptides.

This research was supported in part by National Institutes of Health Grant GM30902, in part by the Office of Naval Research, and in part by a grant from the Department of Science and Technology, India. S.A. was supported by a fellowship of the Council of Scientific and Industrial Research, India.

1. Mueller, P. & Rudin, D. O. (1968) *Nature (London)* **217,** 713–719.
2. Nagaraj, R. & Balaram, P. (1981) *Acc. Chem. Res.* **14,** 356–362.
3. Fox, R. O. & Richards, F. M. (1982) *Nature (London)* **300,** 325–330.
4. Mathew, M. K. & Balaram, P. (1983) *Mol. Cell Biochem.* **50,** 47–64.
5. Hall, J. E., Vodyanoy, I., Balasubramanian, T. M. & Marshall, G. R. (1984) *Biophys. J.* **45,** 233–247.
6. Menestrina, G., Voges, K.-P., Jung, G. & Boheim, G. (1986) *J. Membr. Biol.* **93,** 111–132.
7. Argoudelis, A. D. & Johnson, L. E. (1974) *J. Antibiot.* **27,** 274–282.
8. Rinehart, K. L., Jr., Gaudioso, L. A., Moore, M. L., Pandey, R. C., Cook, J. C., Jr., Barber, M., Sedgwick, R. D., Bordoli, R. S., Tyler, A. N. & Green, B. N. (1981) *J. Am. Chem. Soc.* **103,** 6517–6520.
9. Mellor, I. R., Sansom, M. S. P., Krishna, K. & Balaram, P. (1989) in *Ion Transport*, eds. Keeling, D. & Benham, C. (Academic, New York), pp. 316–318.
10. Krishna, K., Sukumar, M. & Balaram, P. (1990) *Pure Appl. Chem.* **62,** 1417–1420.
11. Egert, E. & Sheldrick, G. M. (1985) *Acta Crystallogr. Sect. A* **41,** 262–268.
12. Karle, I. L., Flippen-Anderson, J., Sukumar, M. & Balaram, P. (1987) *Proc. Natl. Acad. Sci. USA* **84,** 5087–5091.
13. Karle, J. (1968) *Acta Crystallogr. Sect. B* **24,** 182–186.
14. Toniolo, C., Bonora, G. M., Bavoso, A., Benedetti, E., di Blasio, B., Pavone, V. & Pedone, C. (1983) *Biopolymers* **22,** 205–215.
15. Marshall, G. R., Hodgkin, E. E., Langs, D. A., Smith, G. D., Zabrocki, J. & Leplawy, M. T. (1990) *Proc. Natl. Acad. Sci. USA* **87,** 487–491.
16. Karle, I. L. & Balaram, P. (1990) *Biochemistry* **29,** 6747–6756.
17. Schiffer, M. & Edmundson, A. B. (1967) *Biophys. J.* **7,** 121–135.
18. Kaiser, E. T. & Kezdy, F. J. (1984) *Science* **223,** 249–255.
19. IUPAC-IUB Commission on Biochemical Nomenclature (1970) *Biochemistry* **9,** 3471–3479.
20. Stankovic, C. J., Heinemann, S. H. & Schreiber, S. L. (1990) *J. Am. Chem. Soc.* **112,** 3702–3704.
21. Karle, I. L., Flippen-Anderson, J. L., Sukumar, M. & Balaram, P. (1990) *Int. J. Pept. Protein Res.* **35,** 518–526.
22. Karle, I. L., Flippen-Anderson, J. L., Uma, K. & Balaram, P. (1990) *Biopolymers* **29,** 1835–1845.
23. Vogel, H., Nilsson, L., Rigler, R., Voges, K.-P. & Jung, G. (1988) *Proc. Natl. Acad. Sci. USA* **85,** 5067–5071.
24. Miller, C. (1989) *Neuron* **2,** 1195–1205.
25. Richardson, J. S. & Richardson, D. C. (1990) in *Prediction of Protein Structure and the Principles of Protein Conformation*, ed. Fasman, G. D. (Plenum, New York), pp. 1–98.